Plant Archives Volume 20 No. 1, 2020 pp. 187-195 **e-ISSN:2581-6063 (online), ISSN:0972-5210**

EFFECT OF ALTERNATE WATER QUALITY IRRIGATION ON PORE SIZES DISTRIBUTION DURING DRAINAGE IN CLAY LOAM TEXTURE SOIL

Tareq K. Masood and Salloum B. Salim

Department of Soil Sciences and Water Resources, College of Agricultural Engineering Sciences, University of Baghdad, Iraq.

Abstract

A field experiment was conducted at Al-Rashid District-Baghdad, to study the effect of alternate irrigation of fresh and ground water, as a common farming practice, on pore size distribution and parameters of fitted θ(ψ) function of the soil moisture characteristic curve. Fresh water (F, first) and Groundwater (G, second) were added to two (3 m by 3 m) field plots. After the cessation of infiltration cycle, which represents the first cycle, plots were covered to prevent evaporation during 55 days of drainage. At the end of the drainage cycle G was added to the first plot (FG) and F was added to the second plot (GF), which represents the second cycle of alternate use of irrigation water quality. Undisturbed and disturbed soil samples were obtained at the end of each cycle to determine the θ(ψ) relationships at high suction range (0 to -500 cm H_2O), using Tempe pressure cells and low suction range (-1000 to -15000 cm H_2O) using pressure plate apparatus respectively for 10, 30, 50, 70, 90, 110, 130 and 150 cm depths. RETC code was used for parameters estimation of the van Genuchten equation (1980). The dθ/dψ enhanced the calculation of the mean pore size between two consecutive applied suction heads as well as volume fraction (as percent) of total porosity (f) as (dθ/*f*× 100). The results showed that θ measured at high suction range was higher for F compared with G and GF treatment and lower at low suction range. Measured θ values for F was almost the same as measured θ for FG at both high and low suction ranges. Calculated (dθ/*f* ×100) values was greater for F compared with G, FG and GF treatments suggesting more pore spaces was drained for F at the same suction range. Almost similar pore size distribution was found between FG with G and between FG with GF. The (dθ/*f* ×100) values were 70.99, 69.43, 62.57 and 62.07% for F, FG, G and GF treatments with the following descending order: F > FG > G > GF. The results also indicated that more water was retained at pore radius less than 0.198μm which corresponds to -1000cm H_2O suction head value.

Key words : drained pores, soil moisture characteristic curve, fresh water, groundwater.

Introduction

The main consumer of water is the agricultural sector, with global consumption of more than 70% of water (FAO, 2017). In Iraq the agricultural sector consumes about by 71.39 billion m^3/yr to irrigate land area of 5.5 million hectares, while the cultivated land is 3.53 million hectares in 2012, or 64% of the irrigated land. The Iraqi Ministry of Water Resources estimated that a shortfall of 1 billion m^3 of water from neighboring countries would result in 62.5 thousand hectares of irrigated agricultural land, prompting Iraq to import more than 3.52 billion m^3/yr of agricultural virtual water (Ministry of Water Resources of Iraq, 2010 and Abu Zeid and al-Roudi, 2014). As a result of the foreign policies of the neighboring countries of Iraq in cutting off water imports of rivers, it is necessary to think about water resources that are not influenced by international policies. Groundwater is considered an important and strategic storage of water in Iraq and being widely used in many regions for agriculture and industry, as well as for domestic use and drinking in areas away from water resources courses (UNESCO, 2014). Degradation of water quality also depends on the movement of salt water and pollutants from the surface to groundwater through the vadose zone. Many researchers used different irrigation methods to reduce the impact of saline groundwater in crop production and increase yield (Masood, 2015; Masood, 2017 and Mahdi and Masood, 2017). The soil texture and the distribution

***Author for correspondence :** E-mail: tareqmasood@coagri.uobaghdad.edu.iq, sbshassan@gmail.com

Table 1: Some chemical properties of fresh(F) and ground(G) water qualities.

CLASS	SAR	Cl	HCo_3	Mg^{+2}	K^+	Na^+	Ca^{+2}	pH	EC	Water quality
		(Meq/L)							$dS\ m^{-1}$	
C3S1	0.60	8.5	1.2	1.95	0.30	1.25	6.6	7.38	1.2	F
C4S2	7.38	17	1.9	17.4	0.22	32.92	22.4	7.52	7.27	G

of pore sizes have a major role in water content, salt transfer and salinization (Saâdi *et al*., 2018). Effect of salinization increases especially in heavy textured soils, shallow ground water conditions and high irrigation rates. Salts distribution and accumulation in irrigated soils is the outcome of irrigation, evaporation, infiltration and drainage (Rhoades and Handuvi, 1999). Increased salt concentration is problematic in soil structure, especially when sodicity is increased in soil with continuous use of saline irrigation water. The accumulation of mono-valance cations such as sodium and potassium in soil profile, often leads to dispersion of clay, swelling and flocculation. These processes have a negative impact on soil hydraulic properties, infiltration rate and soil moisture characteristic curve. The problem arises for soils already irrigated with saline water followed either by fresh water irrigation or rainfall irrigation during the wet season. Expansion characteristics are affected by repulsive forces between different particles, as well as osmotic forces in small pores and micro-pores resulting from variations in the concentration of saline solution (Musso *et al*., 2003). High concentration of positive (sodium) cations can discourage crystalline expansion (crystalline swelling) and the expansion of the diffused double layer (Liu *et al*., 2018). The thickness of the double layer decreases when the salinity of pore water increases, this in turn reduces swelling pressure (Castellanos *et al*., 2008; Siddiqua *et al*., 2011, 2014). Other studies have indicated that there is no effect of groundwater salinity in the behavior of Clay (Tahtouh *et al*., 2019). The irrigation process enhances the development of the mesh of macro-pore regardless of water quality and resulting in leaching of silt and clay in sandy soils. Leuther *et al*., (2019) noted that poor quality of water causes an increase in pores less than 130 µm. The movement of water and the distribution of pore size in the soil are determined by the electrostatic interactions between the soil and water surfaces that result from the net charge of soil particles. The electrostatic repulsive forces causes the swelling of the soil, which reduces infiltration and the forces of swelling when using the Mg^{+2} solution are much weaker from the use of Na^+ and the determination of the electrical field in the soil depends on soil in filtrability. The low pore sizes of the soil depend on the intensity of the electrostatic forces (Ding *et al*., 2019). Water flows through the area of pores filled with water. When the soil becomes unsaturated the air enters the water instead in the large pores and when the matric potential increases the size of the water-filled pores decreases further (Fredlund and Rahardjo, 1993). Since local irrigation practices in studied area depend on fresh water during abundance (winter season) and ground water during scarcity (summer season), resulting in alternate use of fresh irrigation water and saline ground water, so this study is mainly aimed to determine the impact of alternate use of fresh and salty water on the soil moisture characteristics curve and distribution of pore sizes in clay loam soil.

Table 2: Some physical and chemical properties of the soil.

Depth (cm)	10	30	50	70	90	110	130	150
Sand ($gm\ kg^{-1}$)	245.7	257.9	253.0	184.4		175.8		
Silt ($gm\ kg^{-1}$)	413.4	411.7	394.4	406.2		408.9		
Clay ($gm\ kg^{-1}$)	331.9	330.4	352.6	399.4		415.3		
Soil texture	Clay loam			Silty clay				
Bulk density ($gmcm^{-3}$)	1.32	1.37	1.40	1.43	1.58	1.55	1.58	1.62
$EC_{1:1}$ ($dS\ m^{-1}$)	1.3	1.3	1.9	2.4	3.2	3.4	4.1	3.9
pH	7.1	7.0	7.0	7.2	7.4	7.3	7.4	7.4
CEC ($cmole_c\ kg^{-1}$ soil)	16.7	16.0	14.4	15.2	16.0	22.0	24.0	23.0
$CaCo_3$ (%)	22.3	22.5	17.5	22.1	23.0	22.3	22.5	22.5

Materials and methods

A field experiment was carried out in Al- Rashid area south of Baghdad. The test site is located on 33°04' 28" latitude north and the 44°29'41" longitude is eastward, at an altitude of 29m above sea level, the field soil was classified as sedimentary, with a clay loam texture of 0-0.6m layer and silty clay texture of 0.6-1.6 m layer (Typic, Torrifluevents), Level topography and low salinity. The field was formerly cultivated with wheat. Freshwater (F) was used from the Yusifiyah river which receives water from the Tigris river and groundwater (G) was pumped from a nearby well with water table level at 19m below the soil surface. Some chemical properties of F and G are given in table 1.

Two field plots, (3m by 3m), were selected and surrounded by 0.25m earthen ridges. Three water tanks, each with a capacity of 1 m^3, were placed on board and connected to a distribution system of plastic pipes that receive water from the well and/ or a river. The water application system allows application of a

Table 3: Values of the fitted parameters and R square for Van Genuchten model for different treatments.

Tr.	Parameters	Depth (cm)							
		10	30	50	70	90	110	130	150
F	θ_s	0.449	0.384	0.424	0.422	0.417	0.405	0.404	0.404
	θ_r	0.067	0.121	0.130	0.000	0.134	0.158	0.172	0.169
	α	0.0073	0.0019	0.0017	0.0119	0.0022	0.0023	0.0021	0.0020
	n	1.403	2.832	2.981	1.246	2.518	2.123	2.718	2.760
	R^2	0.955	0.954	0.983	0.970	0.965	0.973	0.965	0.969
	AIC	-71.749	-72.883	-81.433	-70.231	-74.697	-81.840	-78.814	-79.687
FG	θ_s	0.423	0.408	0.386	0.438	0.429	0.392	0.392	0.381
	θ_r	0.111	0.042	0.000	0.152	0.143	0.141	0.157	0.193
	α	0.0038	0.0136	0.0148	0.0021	0.0024	0.0019	0.0016	0.0020
	n	1.650	1.266	1.216	3.106	2.888	3.711	5.537	2.666
	R^2	0.980	0.972	0.978	0.977	0.966	0.986	0.986	0.975
	AIC	-82.579	-81.509	-85.237	-78.609	-74.308	-86.384	-87.468	-87.383
G	θ_s	0.456	0.453	0.393	0.428	0.427	0.407	0.429	0.427
	θ_r	1.26E-05	9.24E-02	1.20E-01	2.67E-02	2.59E-05	4.21E-05	2.23E-01	2.08E-01
	α	0.2378	0.1784	0.0175	0.0189	0.0345	0.0188	0.0019	0.0030
	n	1.113	1.156	1.387	1.174	1.118	1.145	3.610	2.107
	R^2	0.981	0.981	0.990	0.975	0.966	0.912	0.945	0.954
	AIC	-89.703	-91.009	-96.226	-85.586	-85.508	-73.098	-75.529	-78.151
GF	θ_s	0.433	0.433	0.393	0.387	0.443	0.326	0.414	0.447
	θ_r	4.73E-05	0	9.06E-02	1.73E-01	0	1.84E-01	1.98E-01	0
	α	0.0213	0.0291	0.1017	0.0023	0.0432	0.0018	0.0017	0.0213
	n	1.179	1.136	1.230	2.352	1.127	3.905	4.933	1.098
	R^2	0.944	0.956	0.983	0.941	0.973	0.938	0.948	0.941
	AIC	-75.529	-75.170	-92.369	-75.046	-85.816	-82.070	-74.348	-79.899

constant head of 5cm H_2O above plot surface.

At equilibrium (no change in measured water content values), flooding cycle was terminated and the plot was covered to prevent evaporation from the soil surface. Drainage cycle was initiated according to Salem and Saleh, (2008) when ponded water infiltrated through the soil surface. Change in water content was measured at 10, 20, 30, 50, 70, 90, 110, 130 and 150cm depths using soil moisture sensors (Decagon Devices, Pullman Washington) during 55 days while soil profile was undergoing drainage cycle. At the end of drainage cycle the plastic cover was removed and undisturbed and disturbed soil samples were taken from assigned depths. Sampling holes were filled with soil to the nearest bulk density and the plot was left to dry for few days. The plot was then re-flooded again with the other water quality to enhance alternate water quality use in a second cycle. After equilibrium the plot was covered and the drainage cycle was initiated again for another 55days. The experimental setup was performed in a series of four field experiment and was conducted in the following order:

- experiment 1. Plot 1. First cycle fresh water (F).
- experiment 2. Plot 1. Second cycle groundwater after fresh water (FG).
- experiment 3. plot 2. First cycle ground water (G).
- experiment 4. Plot 2. Second cycle fresh water after ground water (GF).

The $\theta(\psi)$ relationships for the studied depths were determined on undisturbed soil samples at suction heads 0, -10, -50, -100, -330 and -500 cm H_2O using tempe pressure cells and on disturbed soil samples at suction heads -1000, -3000, -5000, -10000 and -15000 cm H_2O using pressure plate apparatus. Bulk density was estimated according to Blake and Hartge, (1986). Other samples, from the same depths, were dried, ground and passed through 2 mm diameter sieve, for determining some physical and chemical properties of the field soil as given in table 2.

Van Genuchten model (van Genuchten, 1980) was used to describe the $\theta(\psi)$ relationship as follows:

$$\theta = \theta_r + (\theta_s - \theta_r)\left[1 + (\alpha\psi)^n\right]^m \quad ...1$$

where θ_r is the residual volumetric water content (cm^3cm^{-3}), θ_s is the volumetric content at saturation (cm^3cm^{-3}), θ is the volumetric content measured at any value of suction (cm^3cm^{-3}), ψ is the suction head and α,*n and m* are empirical parameters.

The RETC program was used for parameters estimation of equation 1, using non-linear least square optimizing technique. Pore size distribution was obtained from the capillary equation (Warrick, 2002) which is given by:

$$\psi = \frac{2\gamma \cos\alpha}{\rho_w g r} \qquad ...2$$

where ψ is suction head (cm), γ is the solid–liquid surface tension (71 dyn/cm), α is the solid–liquid contact angle, ρ_w: Water density (g/cm^3), g: gravitational constant (980 cm/sec^2), r: cylindrical pore radius.

On implementing above mentioned values in equation 2 and equating for *r* gives:

$$r = 0.149/\psi \qquad ...3$$

Applied tension values were used to calculate pore sizes range between two consecutive suction heads which correspond to the difference between θ_1 and θ_2 measured at ψ_1 and ψ_2. Effective volume of drained pores was expressed as the difference in water content between two consecutive applied pressure head, ψ_1 and ψ_2, divided by total porosity ($\Delta\theta/f$). Effective pore radius (r) is the mean of pore size range $(r_1+r_2)/2$ (Aoda and Mahdi, 2017):

$$f = 1 - (\rho b / \rho s) \qquad ...4$$

where *f* is the porosity, *ρb* is the soil bulk density (g cm^{-3}), ρ_s is the soil particle density (g cm^{-3}).

Results and Discussion

Fig. 1, shows measured, symbols and non-linear least square fitting using equation 1, solid lines, of volumetric water content (θ) and soil water suction (ψ) for treatments F, FG, G and GF. The θ(ψ) relationship was determined for eight depths, 10, 30, 50, 70, 90, 110, 130 and 150 cm for each treatment. Table 3, shows values of the fitted parameters; θ_s, θ_r, α, n and m besides values of the AIC as a measure of the relative quality of the statistical models. R^2 values of the fitted θ(ψ) function ranged between 0.913 and 0.990, as well as lower AIC (Akaike information criterion, Akaike, 1978) values ranging between -70.23 and -96.226 for the studied depths confirming a significant θ(ψ) relationships. Soil moisture characteristics curve have different treatments F, FG, G and GF, because of the different van Genuchten parameters. Air enter value (α) ranged between 0.0017 and 0.0119 for 50 and 70 cm depths in F treatment, 0.0016

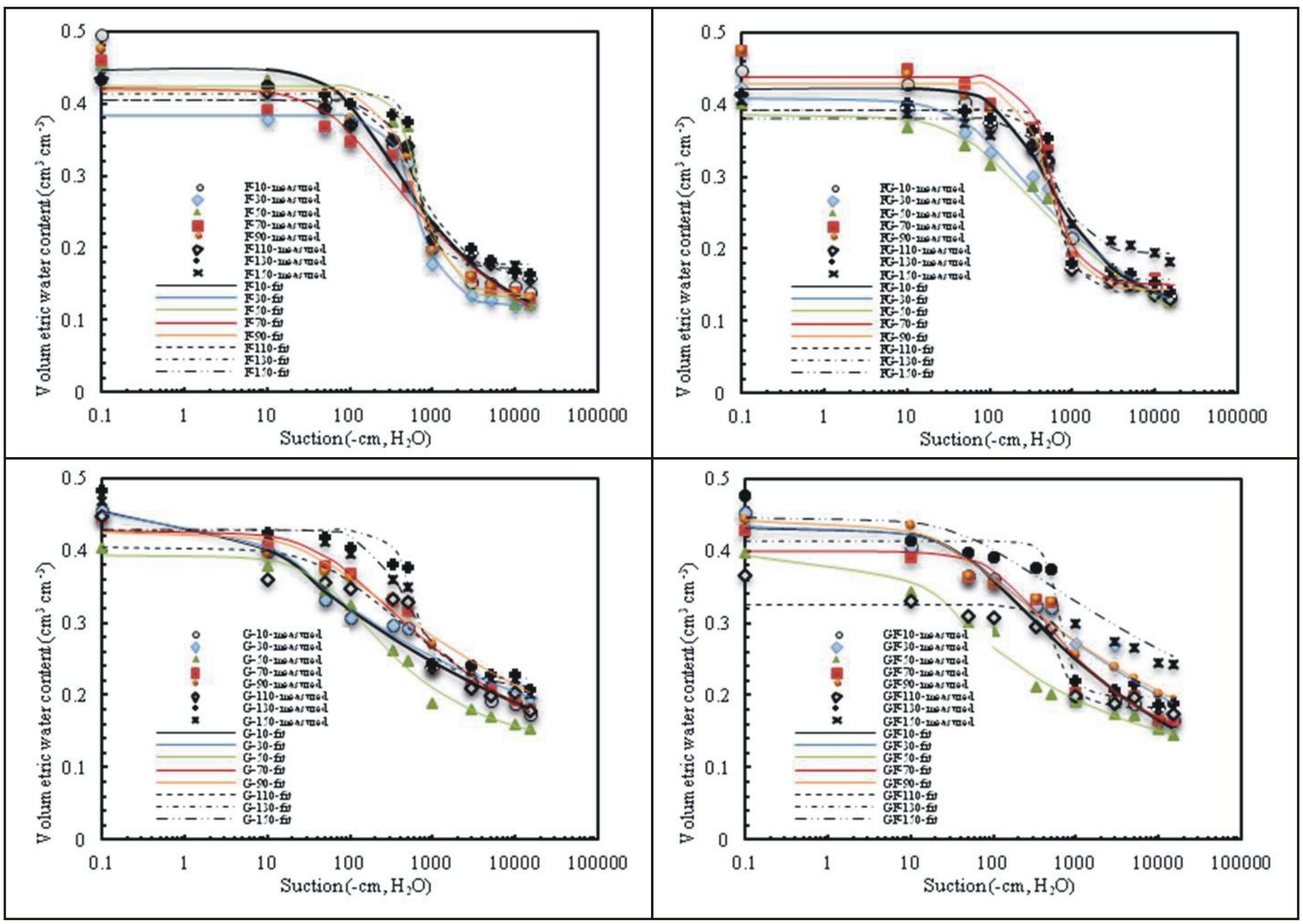

Fig. 1: Measured (symbol) and fitted (solid line) θ(ψ) relationships for F, G, GF, and FG according to van Genuchten model for different depths.

and 0.0148 for 130 and 50 cm depths in FG treatment, 0.0019 and 0.2378 for 130 and 10 cm depths in G treatment and 0.0017 and 0.1017 for 1130 and 50 cm depths in GF treatment respectively which was attributed to the differences in the bulk density (Kool *et al*., 2019). The F treatment had the lowest mean of air enter value compared to FG, G and GF as a result of water quality used in the different treatment. At the same time, Values of *n* ranged between 1.098 and 5.537 for 130 cm and 150cm depths in GF and FG treatment respectively.

Fig. 2, shows 1:1 relationship between measured θ as a function of suction head (soil moisture characteristic curve) For different treatment. At low tension (high water content) the measured volumetric water content for F is higher compared with G and GF, however at high tension (low water content) the measured volumetric water content for F is lower compared with G and GF. No pronounced differences in water content values occurred between F and FG at high and low tension values. Volumetric water content measured at low tension was lower for G compared with FG, but it was higher at high tension values, at the same time, there was no apparent difference between G and GF. Volumetric water content measured at low tension was higher for FG compared with GF, but it was lower at low tension values.

Fig. 2, high significant linear association between

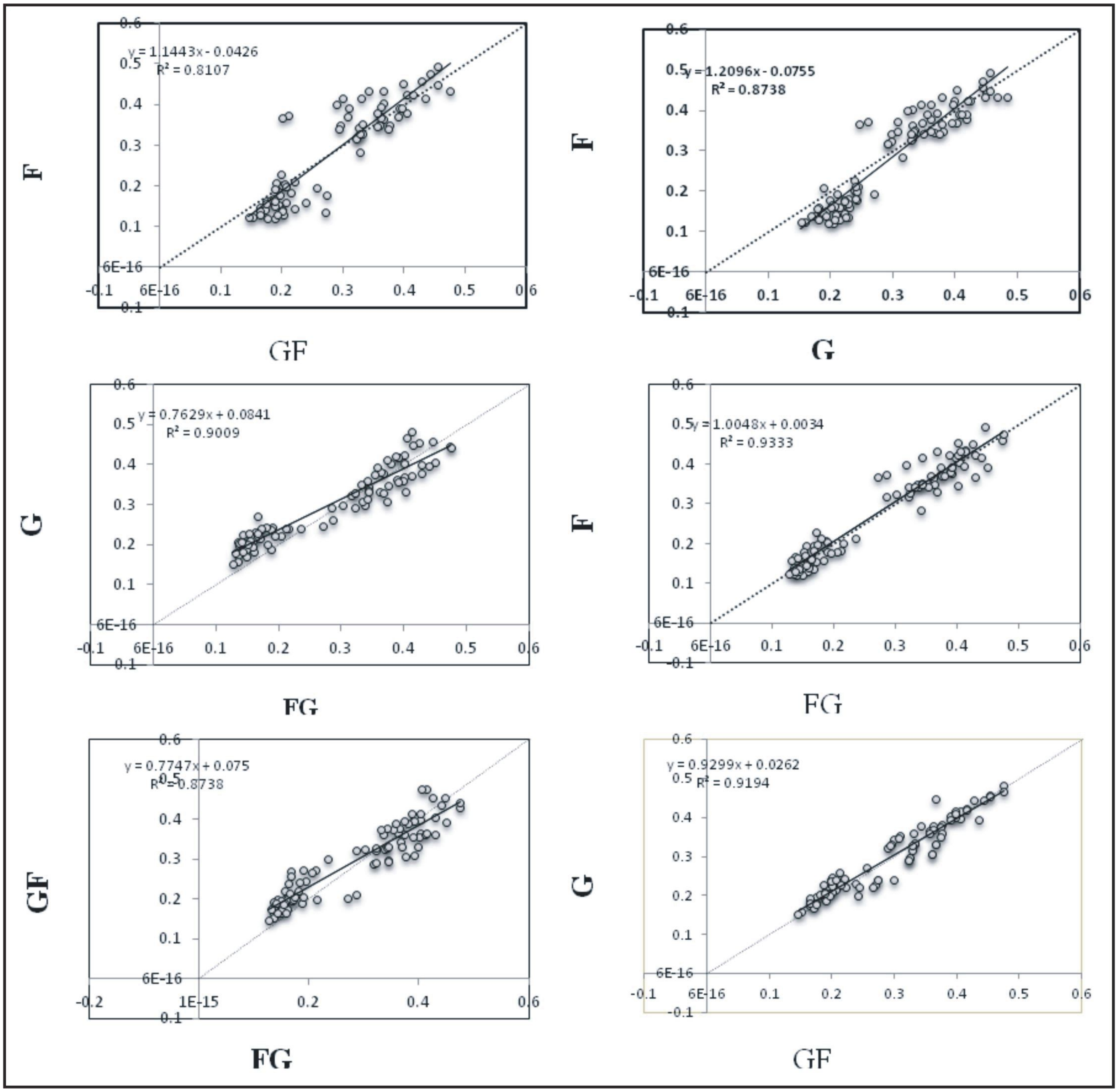

Fig. 2: 1:1 relationship between measured θ as a function of suction head for F, G, GF and FG treatments.

different treatments as evident R^2 values. At low tension the upper layers of soil profile retained more water compared with lower layers as a result of the difference in pore size distribution between the upper and lower layers. In general aggregation is more pronounced in the upper part of soil profile due to biological activities and higher organic matter content, which enhance large pores between and within aggregated soils. As a result the absolute value of volumetric water capacity $d\theta/d\times\psi$ was higher for the upper layers at high tension values, because large pores are first emptied first. Table 2, shows that the bulk density of the lower layers (90-150cm) are greater compared with its value at the upper layers (0-70cm), resulting in lower void ratio at the upper layers. The lower layers retained more water content at low tension values (-1000 to -15000 cm H_2O) due to higher baulk density and greater clay content compared with the upper layers. At the same time, the amount of water retained by the soil when F was added is higher compared with amount of water retained by the soil when G was added first or subsequent alternative cycle (GF).

Fig. 3, shows the pore sizes distribution function as a relationship between the average pores radius (r) between two consecutive tension calculated from equation 2 and the percentage of cumulative effective drained pores ($\Delta\theta/f\times100$) of measured water content values between two

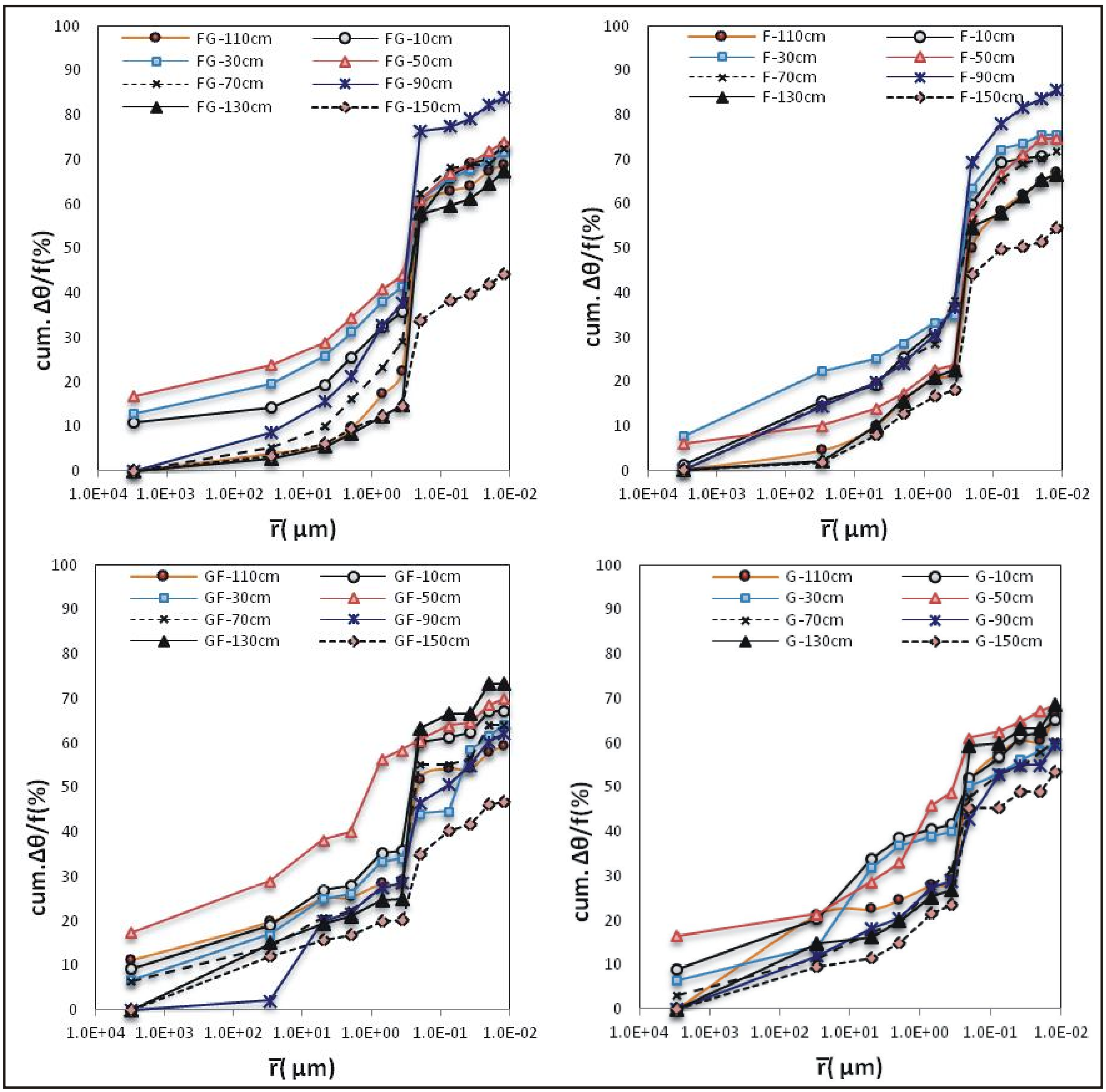

Fig. 3: The relationship between the pore size distribution ($\bar{r}$) and cumulative drained pore percentage.

consecutive tension for 10, 30, 50, 70, 90, 110, 130 and 150cm depths. In the domain of the applied suction head (0 to -15000 cm H_2O) percent of cumulative emptied porosity increased with the decrease in mean pore diameter of all depths and treatments. In addition, there is a clear variation in ($\Delta\theta/f$) ratios, depending on soil depth and irrigation cycle between fresh water and ground water due to the differences in the bulk density, texture, porosity and clay content of different layers.

Fig. 3, shows the pore sizes distribution function as a relationship between the average pores radius at any two consecutive tension (r) calculated from the equation 2 and the percentage of the cumulative drained pore ($\Delta\theta/f$) of the water content values measured for experimental treatments F, FG, G, GF, at 10, 30, 50, 70, 90, 110, 130 and 150 cm depths.

Values of cumulative drained pore ranged between 54.43 and 85.5% for 150 and 90 cm depth in F treatment, 44.23 and 83.98%for 150 and 90 cm depths in FG treatment, 53.30 and 68.48% for 150 and 130 cm depths in G treatment and 46.55 and 73.37% for 150 and 130 cm depths in GF treatment respectively. Regardless of soil depth, the water-free cumulative drained pore of the treatments arranged according to the order following: F> FG> G> GF and values cumulative ($d\theta/f\times100$) were 70.99, 69.43, 62.57 and 62.07% for treatments F, FG, G and GF respectively. The largest pore radius at equilibrium with suction head of -15000 cm H_2O (permanent wilting point) is 1.19×10^{-2} µm. Groundwater treatments retained large part of water within the soil structure and hydrated water surrounding soil particles at radius $\geq 1.98\times10^{-1}$µm which corresponds to suction head value of -1000 cm H_2O and then decrease pore size distribution. These result is an agreement with Higashino and Stefan, (2019) who found more saline water was retained in saline compared with fresh water.

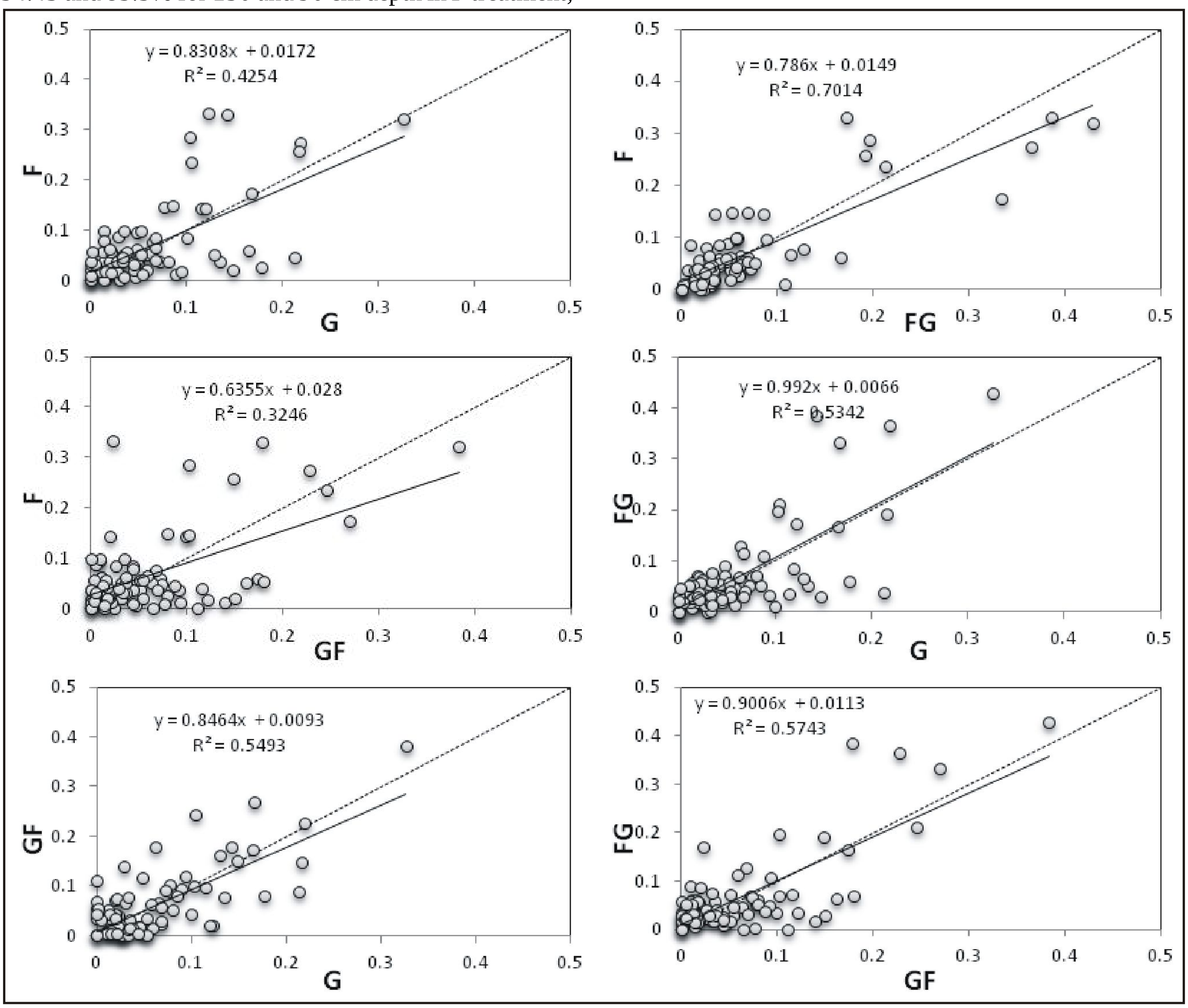

Fig. 4: 1:1 relationship between drained pore size ($d\theta/f$) for different treatment.

At the same time, the drained pore at the high suction head from -0.1 to -500 cm water (the values limits of the field measurements), which corresponds to the average radiuses from 29.5 $\times 10^{-1}$ to 3.59 $\times 10^{-1}$ µm, which were on the following arrangement: G> GF> FG> F, ($d\theta/f \times 100$) reached 33.70, 32.31, 29.99 and 29.08% for treatments of G, GF, FG and F respectively. This confirms that saline ground water led to the development of the macro pore (Wang *et al.*, 2013). Thus having the ability to transfer clay aggregates to layers far from the soil surface (Sumner, 1993; Halliwell *et al.*, 2001). Also Leuther *et al.*, (2019) found that saline water increase in pores less than 130 µm.

Values of drained pore ranged between 0.62 and 33.16% at the radiuses of 3.73×10^{-2} and 1.99×10^{-1}µm for 150 and 50 cm depths in F treatment, 0.22 and 38.57% at the radiuses of 1.99×10^{-2} and 1.99×10^{-1} µm for 70 and 90 cm depths in FG treatment, 0.19 and 32.6% at the radiuses of 7.45×10^{-2} and 1.99×10^{-1} µm for 150 and 130 cm depths in G treatment and 0.28 and 38.29% at the radiuses of 3.59×10^{-1} and 1.99×10^{-1} µm for 150 and 130 cm depths in GF treatment respectively.

The fig. 4, shows 1:1 relationship between different treatments of drained pore, regardless of the depth of the study. The F treatment gave the highest values compared to G, FG and GF. At the same time, the GF treatment gave the highest pore sizes distribution values at the same pore radiuses of G treatment, while the results of pore sizes distribution were associated with treatments of FG, G, FG and GF. The low values of pore size distribution is due to the treatments which took saline groundwater both in the first cycle or second to the effect of salinity itself and this is evident in the relationship between the treatments of GF and G, as there is a slight increase in the values of the pore size distribution in the treatment of GF compared to G treatment.

The increase in pore sizes in the surface layers is due to the role of soil texture and increased sand ratio, which in turn increases the large pores (Al-Rawi, 2008). It can be rated that the decrease in soil moisture at the increase of suction head leads to a decrease and that the decline varies from one treatment to another and from depth to another depending on the pore sizes distribution. therefore, the suction changed from -500 to -1000 cm H_2O, water content decreased significantly for most depths and this is due to the nature of soil texture, while reducing suction and decrease of (r) value, the pores sizes decreased significantly. When the suction was reduced from -5000 to -15,000 cm H_2O, the depths of 110, 130 and 150 cm. Lost highest amount of water compared with the surface depths, especially for the F and FG treatments. The results were different for the groundwater treatments. This is due to the dominance of pore size at these tension, surface area and soil texture such as clay and silt.

References

Abu Zeid, Khalid and Mohammed al-Roudi (2014). The second report on the water situation in the Arab Region -2012. Water Resources programme, CEDARE, Arab Water Council.

Akaike, H. (1978). A Bayesian analysis of the minimum AIC procedure. *Annals of the Institute of Statistical Mathematics*., **30:** 9-14.

Al-Rawi, Sh.S. (2008). The Relation Between The Parameters of Aggregate Stability And Porosity And Water Properties for Soil of Different Texture and Usages. M.Sc. Thesis, College of Agriculture. Baghdad Univ. 117.

Aoda, I.M. and N.T. Mahdi (2017). Analysis Soil Physical Properties. Bookstore for printing publishing and translating. Iraq.

Blake, G.R. and K.H. Hartge (1986). Bulk density. In: Klute A (ed) Methods of Soil Analysis. Part 1. Second edition. *Agron Monogr.,* **9:** 363-375

Castellanos, E., M.V. Villar, E. Romero, A. Lloret and A. Gens (2008). Chemical impact on the hydro-mechanical behaviour of high-density FEBEX bentonite. *Physics and Chemistry of the Earth, Parts A/B/C*., **33(1):** 516-526.

Ding, W., X. Liu, F. Hu, H. Zhu, Y. Luo, S. Li, R. Tian, B. Bao and H. Li (2019). The effect of interactions between particles on soil infiltrability. *Journal of Soils and Sediments*.,1-10. https://doi.org/10.1007/s11368-019-02318-2.

FAO (2017). Water for Sustainable Food and Agriculture, A report produced for the G20 Presidency of Germany. Food and Agriculture Organization of the United Nations, Rome.

Fredlund, D.G. and H. Rahardjo (1993). Soil mechanics for unsaturated soils. New York, NY: John Wiley and Sons, Inc.

Halliwell, D.J., K.M. Barlow and D.M. Nash (2001). A review of the effects of wastewater sodium on soil physical properties and their implications for irrigation systems. *Soil Research*., **39(6):** 1259-1267.

Higashino, M. and H.G. Stefan (2019). Rinsing of Saline Water after Frequent Road Salt Applications from an Unsaturated Sandy Soil by Rainwater Infiltration: Significance of Rainfall Duration. *Journal of Irrigation and Drainage Engineering*., **145(5):** 04019005-1-8.

Kool, D., B. Tong, Z. Tian, J.L. Heitman, T.J. Sauer and R. Horton (2019). Soil water retention and hydraulic conductivity dynamics following tillage. *Soil and Tillage Research*., **193:** 95-100

Leuther, F., S. Schlüter, R. Wallach and H.-J. Vogel (2019). Structure and hydraulic properties in soils under long-term irrigation with treated wastewater. *Geoderma*., **333:** 90-98.

Liu, L.-N., Y.-G. Chen, W.-M. Ye, Y.-J. Cui and D.-B. Wu (2018). Effects of hyperalkaline solutions on the swelling pressure of compacted Gaomiaozi (GMZ) bentonite from the viewpoint of Na^+ cations and OH^- anions. *Applied Clay Science*., **161:** 334-342.

Mahdi, N.T. and T.K. Masood (2017). Water productivity under alternate partial furrow irrigation and organic fertilization for sunflower. *Journal of Agriculture and Veterinary Science (IOSR-JAVS)*., **10:** 01-06.

Masood, T.K. (2015). Irrigation methods and anti-transpiration as related to wheat and water productivity. *Iraqi Journal of Agricultural Science*., **46(6):** 1016-1022.

Masood, T.K. (2017). Effect of irrigation methods on water content distribution, water and corn productivity. *Iraqi Journal of Agricultural Science.,* **48(1):** 178-184.

Ministry of Water Resources of Iraq (2010).Water situation in Iraq. A presentation by the Ministry to the Arab Ministerial Council for Water-Cairo.

Musso, G., E.R. Morales, A. Gens and E. Castellanos (2003). The role of structure in the chemically induced deformations of FEBEX bentonite. *Applied Clay Science*., **23 (1–4):** 229-237.

Rhoades, J.D. and C. Handuvi (1999). Soil salinity assessment-Methods and interpretation of electrical conductivity measurements. Irrigation and drainage paper 57 FAO, Roma, Italy.

Saâdi, M., A. Zghibi and S. Kanzari (2018). Modeling interactions between saturated and un-saturated zones by Hydrus-1D in semi-arid regions (plain of Kairouan, Central Tunisia). *Environmental Monitoring and Assessment.*, **190(3):** 170. 1-18.

Salem, S.B. and A.M. Saleh (2008). Assessment of gravity-drainage unsaturated flow under field conditions for a silty clay loam soil: ii. predicting time rate of change in depth of stored watetr in soil profile. *Iraqi Journal of Agricultural Science.*, **39(4):** 53-62.

Siddiqua, S., G. Siemens, J. Blatz, A. Man and B.F. Lim (2014). Influence of pore fluid chemistry on the mechanical properties of clay-based materials. *Geotechnical and Geological Engineering*., **32(4):** 1029-1042.

Siddiqua, S.S., J.B. Blatz and G.S. Siemens (2011). Evaluation of the impact of pore fluid chemistry on the hydromechanical behaviour of clay-based sealing materials. *Canadian Geotechnical Journal*., **48(2):** 199-213.

Sumner, M.E. (1993). Sodic soils: New perspectives. *Soil Research*., **31(6):** 683-750.

Tahtouh, J., R. Mohtar, A.Assi, P. Schwab, A. Jantrania, Y. Deng and C. Munster (2019). Impact of brackish groundwater and treated wastewater on soil chemical and mineralogical properties. *Science of the Total Environment*., **647:** 99-109

Unesco (2014). Integrated Drought Risk management-Dram national Framework for Iraq an Analysis Report; second edition. march 2014 SC/2014/REPORT/H/1.

Van Genuchten, M.Th (1980). A closed form equation for predicting the hydraulic conductivity of unsaturated. *Soil science society of America journal*., **44:** 892-898.

Wang, L-F., L.L. Wang, X.D. Ye, W.W. Li, X. M. Ren, G.P. Sheng, H.Q. Yu and X.K. Wang (2013). Coagulation kinetics of humic aggregates in mono and di-valent electrolyte solutions *Environmental science & technology.*, **47(10):** 5042-5049.

Warrick, A.W. (2002). Soil Physics Companion. CRC Press LLC, Boca Raton, USA.